J Membrane Biol (2008) 222:55–63
DOI 10.1007/s00232-008-9097-5

ORIGINAL ARTICLES

Altered KCNQ3 Potassium Channel Function Caused by the W309R Pore-Helix Mutation Found in Human Epilepsy

Akira Uehara · Yuki Nakamura · Takao Shioya · Shinichi Hirose · Midori Yasukochi · Kiyoko Uehara

Received: 22 June 2007 / Accepted: 28 January 2008 / Published online: 20 April 2008
© Springer Science+Business Media, LLC 2008

Abstract The second tryptophan (W) residue of the conserved WW motif in the pore helix of many K^+ channel subunit is thought to interact with the tyrosine (Y) residues of the selectivity filter. A missense mutation causing the replacement of the corresponding residues with an arginine (W309R) occurs in KCNQ3 subunits forming part of M-channels. In this study, we examined the functional consequences of the W309R mutation in heterogously expressed KCNQ channels. Homomeric $KCNQ3^{W309R}$ channels lacked KCNQ currents. Heteromeric KCNQ2/$KCNQ3^{W309R}$ channels displayed a dominant-negative suppression of current and a significant modification in gating properties when compared with heteromeric KCNQ3/KCNQ2 channels mimicking the M-channels. A three-dimensional homology model in the W309R mutant indicated that the R side chain of pore helices is too far from the Y side chain of the selectivity filter to interact via hydrogen bonds with each other and stabilize the pore structure. Collectively, the present results suggest that the second W residues of pore helices and their chemical interaction with the Y residues of the selectivity filter are essential for normal K^+ channel function. This pore-helix mutation, if occurs in the brain M channels, could thus lead to a channel dysfunction sufficient to trigger epileptic hyperexcitability.

Keywords Delayed rectifier potassium channel · Brain neuron · Channelopathy · Pore helix · Selectivity filter · Patch clamp

A. Uehara (✉) · Y. Nakamura
Department of Physiology, School of Medicine, Fukuoka University, 45-1, 7-chome Nanakuma, Jonan-ku, Fukuoka 814-0180, Japan
e-mail: ueharaak@fukuoka-u.ac.jp

T. Shioya
Department of Physiology, School of Medicine, Saga University, 1-1, 5-chome, Nabeshima, Saga 849-8501, Japan

S. Hirose
Department of Pediatrics, School of Medicine, Fukuoka University, 45-1, 7-chome Nanakuma, Jonan-ku, Fukuoka 814-0180, Japan

M. Yasukochi
Laboratory of Human Biology, School of Medicine, Fukuoka University, 45-1, 7-chome Nanakuma, Jonan-ku, Fukuoka 814-0180, Japan

K. Uehara
Department of Cell Biology, School of Medicine, Fukuoka University, 45-1, 7-chome Nanakuma, Jonan-ku, Fukuoka 814-0180, Japan

Introduction

The structure of the pore region consisting of the selectivity filter and its surrounding pore helices was determined in bacterial KcsA channels (proton-activated K^+ channels) by X-ray crystallography (Doyle et al. 1998). The side chain of the second tryptophan residue (W68) of the WW motifs located in the pore helices of KcsA channels is considered to interact via hydrogen bonds with that of the tyrosine residue (Y78) of the GYG motifs in the selectivity filter. The amino acid sequences of the WW and GYG motifs are conserved in K^+ channels of many species such as bacterial KcsA channels, *shaker* and human voltage-gated Kv channels. The W68 residue of the WW motif in bacterial KcsA corresponds to the W309 residue of the WW motif in human Kv7.3, i.e., KCNQ3 (KQT-like subfamily, member 3). KCNQ3 and KCNQ2 subunits together generate the muscarinic-regulated potassium currents (M-currents), a slow delayed-rectifier K^+ currents expressed in mammalian

brain neurons which contribute to neuronal excitability control (Brown and Adams 1980; Schroeder et al. 1998; Selyanko et al. 1999; Wang et al. 1998).

The W309 residue in KCNQ3 has been shown to be naturally substituted with arginine (W309R) in benign familial neonatal convulsions (BFNCs), an autosomal dominant generalized epilepsy of human newborns (Hirose et al. 2000). The finding of a missense mutation, W309R, in the epileptic brain M-channels suggests that the W309 residues in pore helices are important to normal K^+ channel function. However, little is known about the dysfunction mechanisms of the W309R mutant channels.

This study was therefore undertaken to characterize the functional consequences of the W309R mutation in heterologously expressed KCNQ channels. In addition, we explored a possible W309R-induced alteration in the pore structure with three-dimensional homology modeling. We aimed to provide insight into the structural and functional significance of a key pore-helix W residue and its possible interaction with other residues in the selectivity-filter in KCNQ K^+ channels. Some of the results have appeared in abstract form (Nakamura et al. 2005).

Materials and Methods

Molecular Biology and Transfections

Full-length cDNAs for KCNQ2 (similar to GenBank accession number AF087453) and KCNQ3 (similar to AF087454) genes were polymerase chain reaction (PCR)-cloned from a rat fetal brain cDNA panel (Clontech, Palo Alto, CA). The cDNAs were subcloned into pCRTOPOII vector (Invitrogen Carlsbad, CA). A nucleotide substitution of KCNQ3 cDNA leading to the pore mutant Trp309Arg (W309R) was introduced into the wild-type construct with the Quick-Change Site-Directed Mutagenesis Kit (Stratagene, La Jolla, CA) on the same vector. All insert sequences as well as mutated sites were confirmed by dideoxyribonucleotide sequencing. The wild-type and mutant cDNA constructs were subsequently transferred to pIRES2-EGFP expression vectors (Clontech). The vectors were transfected in mammalian HEK 293 cells with lipofectamine (Invitrogen). The green fluorescence of coexpressed enhanced green fluorescent proteins (EGFPs) was used as an indicator for successful transfection of KCNQ3. Only fluorescing cells were chosen for electrophysiology.

Western Blotting

Western blot analysis of HEK 293 cell extracts was conducted with KCNQ3 antibodies according to the protocol of Alomone Labs (Jerusalem, Israel). Briefly, proteins (200 µg/lane) from the lysate of KCNQ3 plasmid-transfected and nontransfected cells were resolved by sodium dodecyl sulfate-polyacrylamide gel electrophoresis before transfer onto a nitrocellulose membrane (Amersham Biosciences, Chalfont St. Giles, UK). As an internal standard for equal protein loading, α-tubulin was used (Bassi et al. 2005). Nonfat dry milk (5%; Difco, Detroit, MI) was used as the blocking agent. Incubation was carried out with the first antibody (1:500 dilution) in blocking solution for 2 h and with the secondary antibody of horseradish peroxidase–conjugated goat anti-rabbit (1:10,000 dilution, Amersham Biosciences) in nonfat dry milk for 1 h. Blots were developed by enhanced chemiluminescence (Supersignal; Pierce, Rockford, IL) and exposed on X-ray film (Biomax, Rockville, MD).

Immunocytochemistry

Immunocytochemical experiments on HEK 293 cells expressing KCNQ3 channels were performed according to Ohya et al. (2003). Briefly, HEK 293 cells were seeded onto glass-bottomed dishes. After fixation with paraformaldehyde and permeabilization with Triton X-100, nonspecific binding sites were blocked with phosphate-buffered saline (PBS) and 3% normal donkey serum. Cells were then exposed to anti-KCNQ3 polyclonal antibody (1:50 dilution; Chemicon and Santa Cruz Biotechnology, Santa Cruz, CA) for 12–16 h at 4°C. After removing the excess primary antibodies by repeated washing with PBS, the cells were exposed to Alexa Fluor 546 donkey anti-goat (Santa Cruz Biotechnology) immunoglobulin G antibodies (1:600 dilution; Molecular Probes, Eugene, OR). Excess secondary antibodies were also removed by repeated washing with PBS. Digital images were viewed on a scanning confocal microscope (LSM410; Zeiss, Thornwood, NY). As a negative control, cells were preincubated with excess antigen before the addition of primary antibodies.

Electrophysiology

The whole-cell configuration of the patch-clamp technique was used to measure the potassium currents from HEK 293 cells expressing KCNQ3 channels. The extracellular Tyrode solution consisted of (in mM) NaCl 140, KCl 5.4, Ca 1.8, $MgCl_2$ 0.5, NaH_2PO_4 0.33, HEPES 5 and glucose 5.5 (pH 7.4) titrated with NaOH. The internal solution contained (in mM) K 130, $MgCl_2$ 1, K_2ATP 5, K_2 creatine phosphate 5, aspartic acid 90, EGTA 10 and HEPES 5 (pH 7.4) titrated with KOH (pCa =8). Borosilicate glass electrodes had tip resistances of 1.5–2.5 MΩ when filled with the pipette solution. Membrane currents were amplified and filtered at 1 kHz using an Axopatch 200B (Axon Instruments, Burlingame, CA). The capacitance and series resistance were compensated (60–90%) throughout the experiments. The currents were not leak-subtracted. The

cells were usually held at −70 mV and 1.5 s test voltage pulses in 10 mV increments were applied every 3 s. Currents were sampled at 5 kHz and analyzed using pClamp9 software (Axon Instruments). The current density (pA/pF) was calculated from the ratio between the current size and the cell membrane capacitance, determined by a ramp pulse protocol. All experiments were done at room temperature. Data were expressed as the mean ± standard error of the mean (SEM, n = number of HEK 293 cells). Statistical differences between wild-type and mutant channels in some biophysical parameters were evaluated by Student's t-test. $P < 0.01$ was considered significant.

Three-Dimensional Homology Modeling

Three-dimensional models on the pore helix and the selectivity filter domains of KCNQ3 channels were constructed based on homology with the crystal structure of the corresponding domains of a template KV1.2. SWISS-MODEL was used to generate models of wild-type and mutant KCNQ3 channels. The identity of amino acid residues between KCNQ3 and Kv1.2 was 30.2% in the modeled region.

Results

The Second W Residue in the Pore Helix of K^+ Channels and Missense Mutation

An alignment of the amino acid sequences of the pore region in K^+ channel suunits are shown in Fig. 1A. The WW residues located in the pore helix (blue rectangle) and the GYG residues located in the selectivity filter (red rectangle) are conserved among bacterial KcsA, shaker Kv1.2 and human Kv7.3/KCNQ3 K^+ channel subunits.

Figure 1B illustrates the fundamental protein structure of the selectivity filter and the pore helices in K^+ channels (Doyle et al. 1998). Hydrogen bonds (green line) can interconnect the side chain of the tyrosine (Y) residue (red) in the selectivity filter and that of the second tryptophan (W2) residue (blue) in the pore helix (ribbon) belonging to the neighboring subunit. The hydrogen-bonding network appears to form a structural support for the selectivity filter. A naturally occurring missense mutation (W309R), which is a substitution of the W2 residue in the pore helix by arginine (R) resulting from a nucleotide transition from T 925 to C, was found in a KCNQ3 channelopathy (Hirose et al. 2000).

Protein Expression of W309R KCNQ3 Mutants

No pore mutations of KCNQ were previously reported to interfere with the cell surface expression of channel proteins (Charlier et al. 1998; Schroeder et al. 1998; Schwake et al. 2000). This is plausible because the A-domain tail of the C-terminus is responsible for the normal surface expression of KCNQ channel proteins (Kanki et al. 2004).

Here, we attempted to confirm with Western blot and immunocytochemistry whether the W309R pore-mutant proteins are expressed on the surface membrane of transfected cells. The Western blot experiments revealed that HEK 293 cells transfected with wild-type (KCNQ3) and mutant ($KCNQ3^{W309R}$) plasmids exhibited a similar band

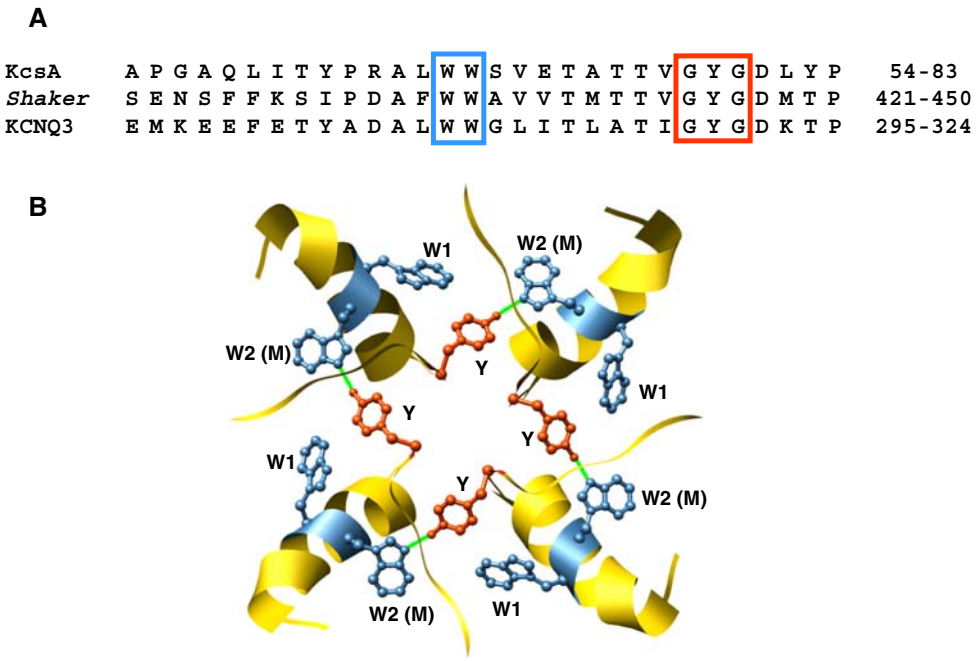

Fig. 1 Location of tryptophan residues in pore helices of K^+ channels. (**A**) Sequence alignments of K^+ channels such as KcsA, *shaker*/Kv1.2 and KCNQ3/Kv7.3. (**B**) Extracellular view of the selectivity filter and the pore helices of channels. In human KCNQ channels, a mutation (M) naturally occurs in the second tryptophan (W2) residues. *Green bar*, Chemical interaction bonding between side chains projected from the two neighboring amino acid residues

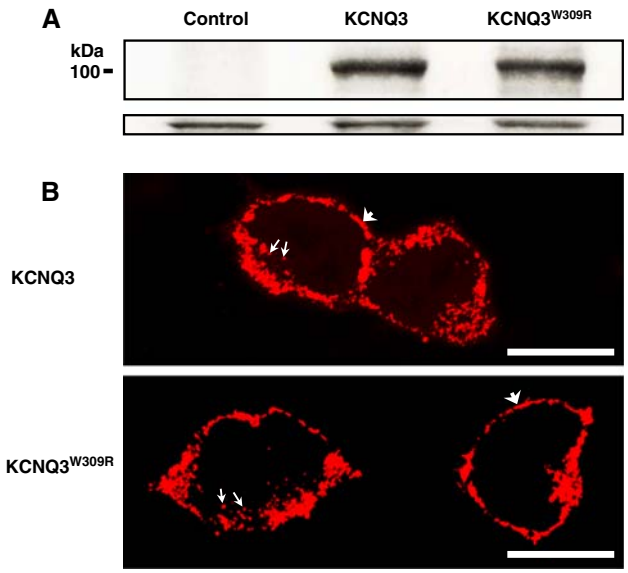

Fig. 2 Protein expression of homomeric KCNQ3 channels in HEK 293 cells. (**A**) Western blotting of nontransfected cells (control), cells transfected with wild-type (KCNQ3) and cells transfected with mutant KCNQ3^{W309R}. Each lane in the lower panel shows the expression of α-tubulin as an internal standard. (**B**) Immunocytochemistry of cells transfected with wild-type KCNQ3 (*upper panel*) and those with mutant KCNQ3^{W309R} (*lower panel*). *Large arrowhead* and *small arrows* point to the immunostained dots in the cell contour and the cytoplasm, respectively. Calibration bar = 10 μm

(Fig. 2A). The single band read approximately 100 kDa of KCNQ3 in molecular weight (Uni Prot/Swiss Prot O88944). The wild-type and mutant KCNQ3 proteins thus appeared to be expressed at the same level in HEK 293 cells, as expected. In contrast, cells not transfected with KCNQ3 plasmids (control) did not show the corresponding band. In addition, confocal images were viewed for KCNQ3-antibody immunofluorescence in HEK 293 cells (Fig. 2B). The cell contour and the cytoplasm of the transfected cells were positively immunostained in red. Cells expressing mutant channels were similar in immunocytochemical appearance to cells expressing wild-type channels. These results collectively suggest that the W309R mutation at the pore helix of KCNQ3 channels does not impair normal protein expression in HEK 293 cells.

Whole-Cell Currents from Homomeric KCNQ3^{W309R} Channels

Membrane currents were obtained from homomeric wild-type KCNQ3 (Fig. 3A) and mutant KCNQ3^{W309R} (Fig. 3B) channels expressed in HEK 293 cells. KCNQ3 generated typical time- and voltage-dependent outward KCNQ currents, whereas neither KCNQ3^{W309R} (Fig. 3B) nor nontransfectants (data not shown) showed such currents. Current densities (pA/pF) of nontransfectants (control), KCNQ3, KCNQ2 and KCNQ3^{W309R} were subsequently calculated by dividing the peak current at the end of the test pulse of +40 m*V* (called "late currents") by the cell capacitance (Fig. 3C). The mutant KCNQ3^{W309R} channels were strikingly different in current density from wild-type KCNQ3 channels (*t*-test, $P < 0.01$) but not significantly different from nontransfectants (*t*-test, $P > 0.01$).

To examine whether the W309 residue is essential to maintain normal KCNQ channel function, we performed more site-directed mutagenesis experiments on the W309 residue which was replaced by the other aromatic amino acids of phenylalanine (F) and tyrosine (Y) (Fig. 3B, D).

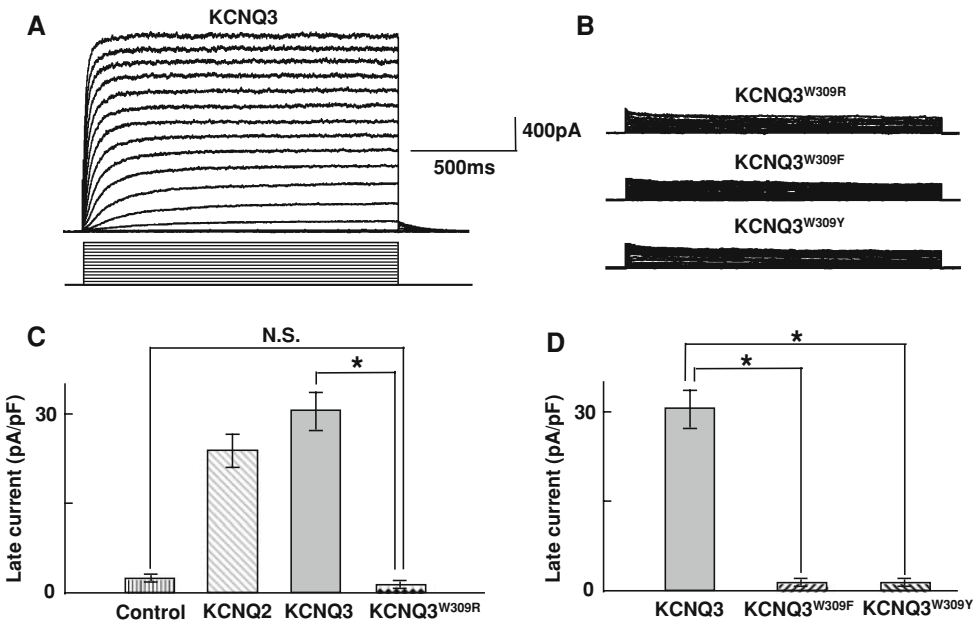

Fig. 3 Whole-cell currents obtained from homomeric channels. (**A**) Representative current traces from wild-type KCNQ3 channels. (**B**) Representative current traces from mutant channels of KCNQ3^{W309R}, KCNQ3^{W309F} and KCNQ3^{W309Y}. (**C**) Current densities of late currents in nontransfectants (control), KCNQ2, KCNQ3 and KCNQ3^{W309R} (each $n = 26$). (**D**) Current densities of late currents in wild-type KCNQ3 ($n = 26$), KCNQ3^{W309F} ($n = 18$) and KCNQ3^{W309Y} ($n = 19$). Asterisks and N.S., statistically significant and nonsignificant differences, respectively

At physiologically neutral pH, all of W, F and Y residues are nonpolar and neutral with no net charge but R residues possess a positive charge. No KCNQ currents were generated in homomeric channels of either KCNQ3^{W309F} or KCNQ3^{W309Y}, as well as KCNQ3^{W309R}. KCNQ3^{W309F} and KCNQ3^{W309Y} showed a striking difference in current density from wild-type KCNQ3 (*t*-test, $P < 0.01$). Thus, neither Fnor Y residue could replace of the W309 residue to maintain the normal channel function.

Whole-Cell Currents from Heteromeric KCNQ2/KCNQ3^{W309R} Channels

Since brain M-channels comprise two kinds of subunits, such as KCNQ3 and KCNQ2, we characterized membrane currents from heteromers coexpressed with the two subunits (Fig. 4A). KCNQ2/KCNQ3 yielded robust currents, whereas KCNQ2/KCNQ3^{W309R} yielded markedly suppressed currents. The current-voltage relationship of the late currents revealed that KCNQ2/KCNQ3^{W309R} was far smaller (*t*-test, $P < 0.01$) at almost all test potentials in current density than KCNQ2/KCNQ3 (Fig. 4B). The tail currents of KCNQ2/KCNQ3^{W309R} (Fig. 4C) showed a considerable reduction of about 70% of KCNQ2/KCNQ3 at a test pulse of +50 m*V* ($n = 10$) (data not shown). Thus, the W309R mutation reduced the currents of the heteromeric channel in a dominant-negative manner (defined by a current reduction of >50%).

The measurable currents of heteromeric KCNQ2/KCNQ3^{W309R} enabled us to make a comparison in gating properties between wild-type and mutant KCNQ channels. The voltage/activation curves were derived from standard analysis of the tail currents in the heteromeric channels (Fig. 4C) with the Boltzmann equation: $I = 1/[1 + \exp(V_{half} - V)/k]$ (Fig. 4D). The half-activating voltage (V_{half}) and the slope factor (k) of the heteromeric channels were −29.6 and 13.5 m*V*/*e*-fold, respectively, in KCNQ2/KCNQ3^{W309R} and −37.1 and 11.6 m*V*/*e*-fold, respectively, in KCNQ2/KCNQ3. In addition, V_{half} and k of the homomeric channels were −46.9 and 7.1 m*V*/*e*-fold, respectively, in KCNQ3 (gray solid lines) and −9.6 and 17.4 m*V*/*e*-fold, respectively, in KCNQ2 (gray dashed line). These four kinds of KCNQ channels were significantly different from one another in V_{half} values (*t*-test, $P < 0.01$). The voltage dependence of KCNQ2/KCNQ3^{W309R} was shallower and its voltage/activation curve shifted slightly toward positive potential when compared with KCNQ2/KCNQ3. The voltage/activation curve of KCNQ2/KCNQ3^{W309R} was distant from either curve of KCNQ2 and KCNQ3 homomers.

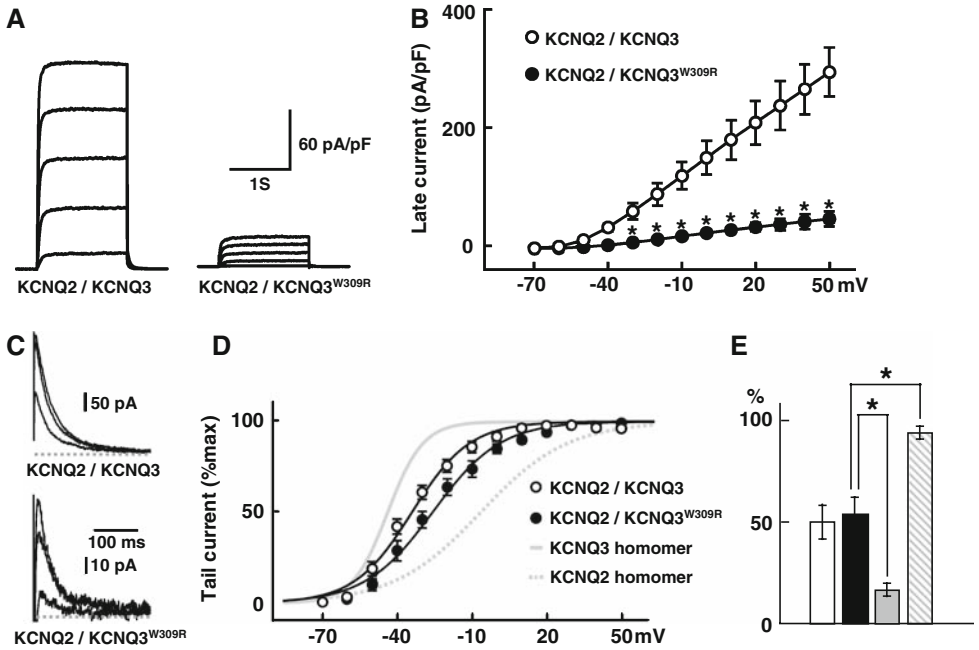

Fig. 4 Whole-cell currents obtained from heteromeric KCNQ2/KCNQ3^{W309R} channels. (**A**) *Left panel*: Representative currents of KCNQ2/KCNQ3. *Right panel*: Representative current traces of KCNQ2/KCNQ3^{W309R}. (**B**) Current-voltage relationship of the late currents of KCNQ2/KCNQ3 ($n = 10$) and KCNQ2/KCNQ3^{W309R} ($n = 11$). (**C**) Representative tail-current traces of KCNQ2/KCNQ3 (*upper panel*) and KCNQ2/KCNQ3^{W309R} (*lower panel*). *Dashed line* denotes zero current level. (**D**) Voltage/activation curves of KCNQ2/KCNQ3 ($n = 11$), KCNQ2/KCNQ3^{W309R} ($n = 13$), KCNQ3 homomer ($n = 15$) and KCNQ2 homomer ($n = 15$). (**E**) Sensitivity to TEA of KCNQ2/KCNQ3 (*white bar*, $n = 10$), KCNQ2/KCNQ3^{W309R} (*black bar*, $n = 9$), KCNQ3 homomer (*gray bar*, $n = 9$) and KCNQ2 homomer (*hatched bar*, $n = 8$). * $P < 0.01$

The potassium channel blocker tetraethylammonium (TEA) is known to be useful for discriminating among KCNQ2 homomers, KCNQ3 homomers, and KCNQ2/KCNQ3 heteromers owing to their differential drug sensitivity (Soldovieri et al. 2006). Soldovieri et al. (2006) compared TEA sensitivities of KCNQ2/KCNQ3 and KCNQ2/KCNQ3^{W309R} heteromers with those of KCNQ2 and KCNQ3 homomers (Fig. 4E). TEA sensitivity is expressed as percent of blockade of the currents recorded at +20 m*V* by perfusion of 10 mM TEA for 3 min. KCNQ2/KCNQ3^{W309R} displayed a significant difference (*t*-test, $P < 0.01$) from KCNQ3 and KCNQ2 homomers. The significant differences among KCNQ2/KCNQ3^{W309R}, KCNQ3 and KCNQ2 in TEA sensitivity (Fig. 4E), as well as in the voltage dependence of current activation (Fig. 4D), imply that the KCNQ2/KCNQ3^{W309R} currents obtained reflect the characteristics of the currents generated by the heteromeric assembly of KCNQ2 and KCNQ3^{W309R} subunits. Whether the coexpression of KCNQ2 and KCNQ3 subunits yields a mixture of subunit combinations (4KCNQ2, 3KCNQ2/1KCNQ3, 2KCNQ2/2KCNQ3, 1KCNQ2/3KCNQ3, 4KCNQ3), however, remains to be examined. Possible stoichiometry of coexpressed subunits might be resolved in future experiments by comparison with currents from the tandem construct of KCNQ2–KCNQ3.

Current activation kinetics during a depolarizing stimulation was compared between the two heteromeric channels of KCNQ2/KCNQ3 and KCNQ2/KCNQ3^{W309R}. The membrane currents elicited by a test pulse of +50 m*V* were normalized with the maximum amplitude at the end of the test pulse and best fitted with a double exponential function (Fig. 5A). The time constants (τ_{fast}, τ_{slow}) and relative contribution (As/[As+Af]) of their slow-amplitude component (As) for activation were larger in KCNQ2/KCNQ3^{W309R} than in KCNQ2/KCNQ3 (Fig. 5B). Thus, the activation kinetics of KCNQ2/KCNQ3^{W309R} was significantly slower than that of KCNQ2/KCNQ3 (*t*-test, $P < 0.01$).

We examined whether the cation permeability of KCNQ channels to monovalent cations such as Rb^+ and Cs^+ is altered by the W309R mutation of KCNQ3. A shift in reversal potential (data not shown) was measured in heteromeric KCNQ2/KCNQ3 and KCNQ2/KCNQ3^{W309R} channels, which generate detectable currents, under bi-ionic conditions with 15 mM cation in the external solution and 150 mM K^+ in the internal solution. The relative Rb^+ permeability (P_{Rb}/P_k), which was calculated from the Goldman-Hodgkin-Katz equation, was 0.69 ± 0.05 and 0.70 ± 0.04 in KCNQ2/KCNQ3 ($n = 8$) and KCNQ2/KCNQ3^{W309R} ($n = 10$), respectively. The relative Cs^+ permeability (P_{Cs}/P_k) was 0.082 ± 0.005 and 0.080 ± 0.04 in KCNQ2/KCNQ3 ($n = 7$) and KCNQ2/KCNQ3^{W309R} ($n = 8$), respectively. Thus, we failed to detect any significant alteration by the W309R mutation of KCNQ3 in Rb^+ and Cs^+ permeability.

Whole-Cell Currents from Heteromeric KCNQ2/KCNQ3/KCNQ3^{W309R} Channels

To mimic the heterozygous condition of the epileptic patient, we performed functional analysis on more complex heteromers obtained during triple coexpression of KCNQ2/

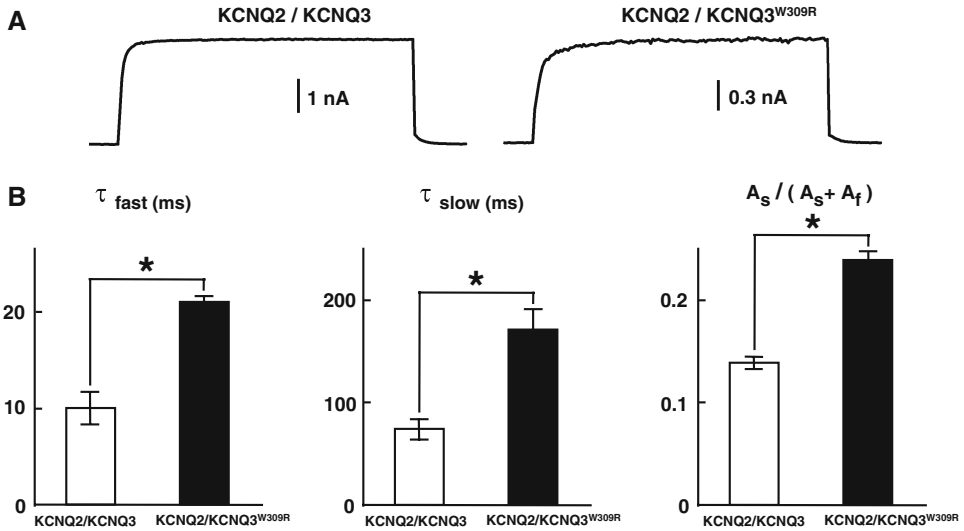

Fig. 5 Activation kinetics of heteromeric KCNQ2/KCNQ3^{W309R} channels. (**A**) *Left panel*: Representative normalized current traces from KCNQ2/KCNQ3. *Right panel*: Representative normalized current traces from KCNQ2/KCNQ3^{W309R}. *Gray curves* illustrate exponential-fitting curves of current activation. (**B**) *Left panel*: Fast time constants, τ_{fast}, of KCNQ2/KCNQ3 ($n = 11$) and KCNQ2/KCNQ3^{W309R} ($n = 12$). *Middle panel*: Slow time constants, τ_{slow}, of the same heteromeric channels. *Right panel*: Relative contribution, $A_s/(A_s + A_f)$, of the slow-amplitude components, A_s, of the same heteromeric channels. * $P < 0.01$

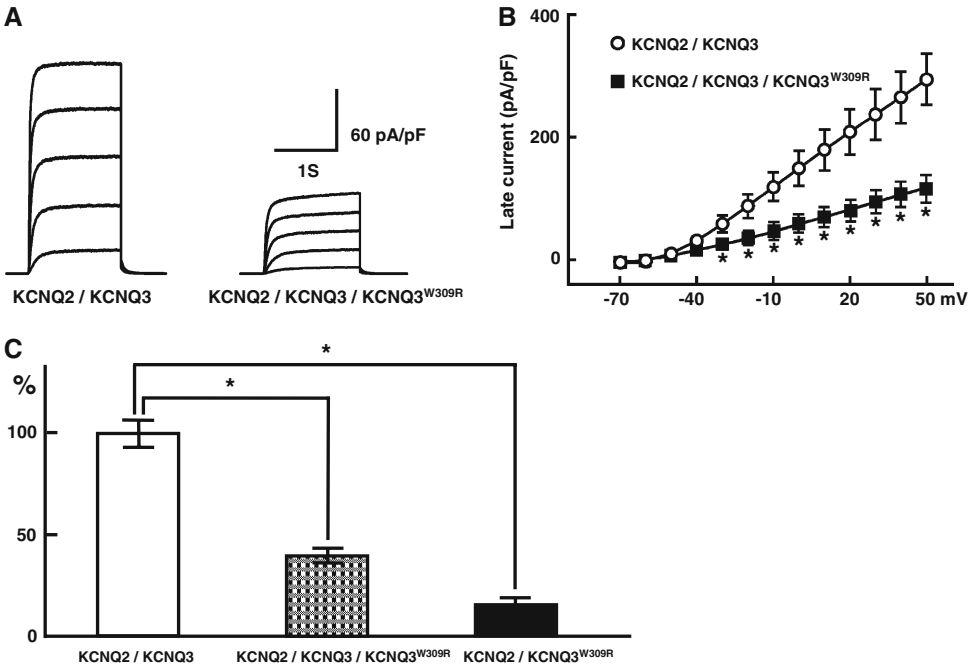

Fig. 6 Whole-cell currents obtained from heteromeric KCNQ2/KCNQ3/KCNQ3^{W309R} channels. (**A**) Representative current traces of KCNQ2/KCNQ3 and KCNQ2/KCNQ3/KCNQ3^{W309R}. (**B**) Current-voltage relationship of the late currents of KCNQ2/KCNQ3 ($n = 10$) and KCNQ2/KCNQ3/KCNQ3^{W309R} ($n = 8$). (**C**) Current densities of late currents at the test pulse of +40 m*V* in KCNQ2/KCNQ3 ($n = 10$), KCNQ2/KCNQ3/KCNQ3^{W309R} ($n = 8$) and KCNQ2/KCNQ3^{W309R} ($n = 11$). * $P < 0.01$

KCNQ3/KCNQ3^{W309R} subunits at their respective plasmid ratio of 1:0.5:0.5 (Fig. 6). KCNQ2/KCNQ3/KCNQ3^{W309R} was significantly decreased (*t*-test, $P < 0.01$) in current density compared to KCNQ2/KCNQ3 over the test potentials examined (Fig. 6A, B). The current density obtained from the late currents was statistically compared at the test pulse of +40 m*V* between KCNQ2/KCNQ3 and KCNQ2/KCNQ3/KCNQ3^{W309R} (Fig. 6C). Consequently, the currents recorded upon KCNQ2/KCNQ3 / KCNQ3^{W309R} expression were suppressed by about 60% when compared with KCNQ2/KCNQ3-expressing cells. Thus, this mutation in the pore helix exerted a dominant-negative effect in not only KCNQ2/KCNQ3^{W309R} but also KCNQ2/KCNQ3/KCNQ3^{W309R}. Boltzmann's voltage/activation curve of KCNQ2/KCNQ3/KCNQ3^{W309R} was interposed between that of KCNQ2/KCNQ3 and that of KCNQ2/KCNQ3^{W309R} in Fig. 4D (data not shown).

Discussion

Dysfunction of Homomeric KCNQ3^{W309R} and Heteromeric KCNQ2/KCNQ3^{W309R} Channels

The present study demonstrates a remarkable dysfunction of KCNQ3 channels by the W309R mutation found in a human K^+ channelopathy. W309R is not a nonsense, deletion, frameshift or splicing error mutation but a missense mutation in which a single amino acid residue of the protein is merely substituted by the other residue. This missense mutation, which affects the second W residues of the WW motif in pore helices, abolished KCNQ3 currents in homomeric configuration (Fig. 3). This abolishment in KCNQ3 currents is likely due to the loss of function of the channel molecules expressed on the cell surface (Fig. 2B), although trafficking defects of the channel molecules cannot be completely ruled out. In the case of heteromeric channels, like brain M-channels, obtained during double coexpression of KCNQ3 and KCNQ2 subunits, this mutation caused a partial and dominant-negative current suppression (Fig. 4A, B). Gating properties of heteromeric KCNQ2/KCNQ3^{W309R} channels were significantly altered by the W309 mutation (Figs. 4C, D and 5). In contrast, it was previously reported that gating properties are unaffected by BFNC-causing pore mutations identified thus far in KCNQ3 channels (Singh et al. 2003). Here, we propose that the second W residues in pore helices are essential for functional delayed-rectifier KCNQ channels.

Dominant-Negative Effect in Heteromeric KCNQ2/KCNQ3/KCNQ3^{W309R} Channels Mimicking the Situation in a Heterozygous Patient

A BFNC-associated pore mutation (G310V) was demonstrated to reduce the heteromeric channel currents during triple coexpression with mutant KCNQ3/wild-type KCNQ3/wild-type KCNQ2 subunits in frog oocytes, by only 20% compared with wild-type KCNQ2/wild-type KCNQ3 (Schroeder et al. 1998). This mutation thus exerted a non-dominant-negative, i.e., a recessive, effect (defined by a current reduction <50%). However, an

artificial pore mutation (G318S), not associated with BFNC, was shown to exert a dominant-negative effect on heteromeric channels of mutant KCNQ3/wild-type KCNQ3/wild-type KCNQ2 subunits (Schroeder et al. 1998). Therefore, it is seemingly possible that some other pore mutations affecting different amino acid residues or introducing a different substitution, have a dominant negative effect.

In the present study, we conducted a functional analysis using HEK 293 cells coexpressing triple KCNQ2/KCNQ3/KCNQ3^{W309R} subunits to mimick the heterozygous condition of the patient, although it is better to use frog oocytes than HEK 293 cells for quantitative heteromultimer expression (Fig. 6). KCNQ2/KCNQ3/KCNQ3^{W309R} reduced current in a dominant-negative manner by >50% compared with wild-type KCNQ2/KCNQ3 (Fig. 6C). This effect in our W309R BFNC-associated mutant contrasts with the recessive effect in other BFNC-associated KCNQ3 (Schroeder et al. 1998) and KCNQ2 (Schroeder et al. 1998; Biervert et al. 1998) mutants. We believe that some BFNC-associated KCNQ pore mutants including KCNQ3^{W309R} can display a dominant-negative current suppression in the heteromeric channel.

No Effect of W309R Mutation on Permeation Properties of KCNQ2/KCNQ3 Channels

In our experiments, we failed to detect any significant difference in the permeation properties to monovalent cations such as Rb^+ and Cs^+ between KCNQ2/KCNQ3 and KCNQ2/KCNQ3^{W309R} currents (see "Results"). Only the second W residues belonging to KCNQ3 subunits of all WW motifs derived from both KCNQ2 and KCNQ3 subunits are substituted in the case of KCNQ2/KCNQ3^{W309R} heterotetramers. It is worthy of note that the second W residues belonging to KCNQ2 subunits and all the first W residues of KCNQ2 and KCNQ3 subunits remain in the tetramer channels. This partial substitution of W residues in pore helices would thus be insufficient to alter the permeation properties of heteromeric KCNQ2/KCNQ3^{W309R} channels.

Impairments of the Chemical-Bonding Interaction Between the Selectivity Filter and the Pore Helix by W309R Mutation

We built homology models of the selectivity filter and its surrounding pore helix in homomeric KCNQ3 channels to hypothesize a possible structural alteration caused by the W309R pore mutation (Fig. 7). In our model, the distance between the W2 and Y side chains was 2.8 angstrom in wild-type KCNQ3 homomers (Fig. 7A), while that between the R and Y side chains was 6.5 angstrom (Fig. 7B). Therefore, the distance between the R and Y side chains was more than twice as great as that between the W and Y side chains in wild-type KCNQ3 homomers.

The side chains of the W and R residues possess an indoyl and a guanidyl group, respectively. These two groups can be hydrogen donors. In terms of hydrogen donors, not only W but also R side chains potentially form a hydrogen bond, with a hydroxyl group of the Y side chain functioning as a hydrogen acceptor. However, it depends on the distance between the W/R and Y side chains whether hydrogen bonds are made or not between them. Hydrogen bonds are likely to be formed as illustrated in Fig. 1B, judging from the short distance of 2.8 angstrom between the W2 and Y side chains (Fig. 7A). In the case of mutant KCNQ3^{W309R} homomers, on the contrary, the R side chains appear to be too far (6.5 angstrom, considerably larger than 3 angstrom) from the Y side chains to form hydrogen bonds between them (Fig. 7B). This interference of the chemical-bonding interaction by the W309R mutation may stabilize the structure of the selectivity filter and its surroundings to cause the channel dysfunction.

Complete dysfunction in homomeric KCNQ3^{W309R} channels (Fig. 3B, C) is possibly due to the lack of all four hydrogen bonds between the R309 side chains from the pore helices of KCNQ3^{W309R} subunits and the Y side chains from the selectivity filter of neighboring KCNQ3^{W309R} subunits. On the other hand, the moderate dysfunction in heteromeric KCNQ2/KCNQ3^{W309R} channels (Fig. 4A) is possibly due to the hydrogen bonds partly remaining between the W309 side chains from wild-type

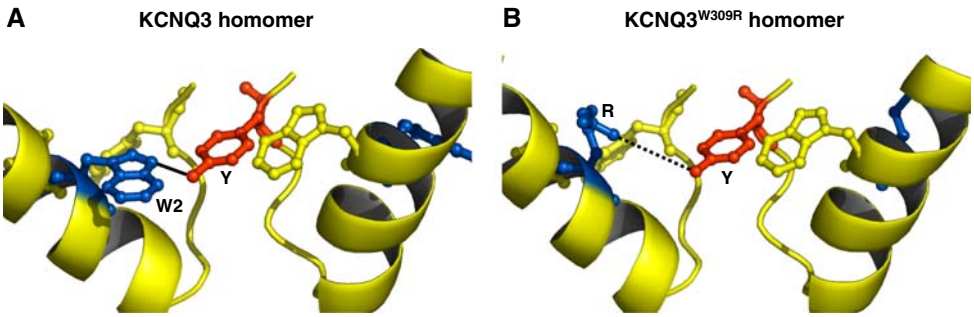

Fig. 7 Three-dimensional homology models around the selectivity filter and pore helices in homomeric KCNQ3 channels. (**A**) Wild-type KCNQ3. (**B**) Mutant KCNQ3^{W309R}. *Yellow ribbons* show pore helices. Symbols W2, Y and R represent an amino acid residue of the second tryptophan, tyrosine and arginine, respectively

KCNQ2 subunits and the Y side chains from neighboring $KCNQ3^{W309R}$ subunits.

Pathophysiological Implication of the W309R Mutation in Brain M-Channels

KCNQ3 subunits form heterotetramers with either KCNQ2 (Schroeder et al. 1998; Selyanko et al. 1999; Wang et al. 1998), KCNQ4 (Kubisch et al. 1999) or KCNQ5 (Kananura et al. 2000; Lerche et al. 2000; Schroeder et al. 2000) subunits to generate brain M-currents. When a pore mutation naturally occurs in KCNQ3 subunits of in vivo heterotetrameric channels composed of KCNQ3 common subunits and KCNQ2, -4 or -5 replaceable subunits, membrane currents are likely to flow due to the intact subunits of wild-type KCNQ2, -4 or -5. The W309R mutation occurring in only the KCNQ3 subunits could thus result in a partial reduction of brain M-currents. This partial current reduction by the autosomal dominant BFNC-causing W309R mutation should suffice to cause hyperexcitability in human epilepsy phenotype.

In conclusion, our present study first describes functional and possible structural impairments caused by the W309R mutation of KCNQ3 associated with human epilepsy. These results suggest that the second W residues of pore helices and their hydrogen-bonding interaction with the Y residues of the selectivity filter are essential for normal K^+-channel pore function. The pore-helix mutation, if it occurs naturally in M-channels, is likely to lead to the potassium channelopathy.

Acknowledgements The authors thank A. Hamachi and M. Yonetani for technical assistance and Drs. S. Matsuoka, T. Ishii and N. Aoki for valuable comments. This work was supported by a Grant-in Aid for Scientific Research from the Ministry of Education, Science and Culture of Japan.

References

Bassi MT, Balottin U, Panzeri C, Piccinelli P, Castaldo P, Barrese V, Soldovieri MV, Miceli F, Colombo M, Bresolin N, Borgatti R, Taglialatela M (2005) Functional analysis of novel KCNQ2 and KCNQ3 gene variants found in a large pedigree with benign familial neonatal convulsions (BFNC). Neurogenetics 6:185–193

Biervert C, Schroeder BC, Kubisch C, Berkovic SF, Propping P, Jentsch TJ, Steinlein OK (1998) A potassium channel mutation in neonatal human epilepsy. Science 279:403–406

Brown DA, Adams PR (1980) Muscarinic suppression of a novel voltage-sensitive K^+ current in a vertebrate neuron. Nature 283:673–676

Charlier C, Singh NA, Ryan SG, Lewis TB, Reus BE, Leach RJ, Leppert M (1998) A pore mutation in a novel KQT-like potassium channel gene in an idiopathic epilepsy family. Nature Genet 18:53–55

Doyle DA, Morais Cabral J, Pfuetzner RA, Kuo A, Gulbis JM, Cohen SL, Chait BT, MacKinnon R (1998) The structure of the potassium channel: molecular basis of K^+ conduction and selectivity. Science 280:69–77

Hirose S, Zenri F, Akiyoshi H, Fukuma G, Iwata H, Inoue T, Yonetani M, Tsutsumi M, Muranaka H, Kurokawa T, Hanai T, Wada K, Kaneko S, Mitsudome A (2000) A novel mutation of KCNQ3 (C925T–>C) in a Japanese family with benign familial neonatal convulsions. Ann Neurol 47:822–826

Kananura C, Biervert C, Hechenberger M, Engels H, Steinlein OK (2000) The new voltage gated potassium channel KCNQ5 and neonatal convulsions. Neuroreport 11:2063–2067

Kanki H, Kupershmidt S, Yang T, Wells S, Roden DM (2004) A structural requirement for processing the cardiac K^+ channel KCNQ1. J Biol Chem 279:33976–33983

Kubisch C, Schroeder BC, Friedrich T, Lütjohann B, El-Amraoui A, Marlin S, Petit C, Jentsch TJ (1999) KCNQ4, a novel potassium channel expressed in sensory outer hair cells, is mutated in dominant deafness. Cell 96:437–446

Lerche C, Scherer CR, Seebohm G, Derst C, Wei AD, Busch AE, Steinmeyer K (2000) Molecular cloning and functional expression of KCNQ5, a potassium channel subunit that may contribute to neuronal M-current diversity. J Biol Chem 275:22395–22400

Nakamura Y, Shioya T, Yasukochi M, Imanaga I, Uehara A (2005) Dysfunction by a missense mutation of voltage-gated K channel KCNQ3. J Physiol Sci Suppl 55:S126

Ohya S, Sergeant GP, Greenwood IA, Horowitz B (2003) Molecular variants of KCNQ channels expressed in murine portal vein myocytes: a role in delayed rectifier current. Circ Res 92:1016–1023

Schroeder BC, Kubisch C, Stein V, Jentsch TJ (1998) Moderate loss of function of cyclic-AMP-modulated KCNQ2/KCNQ3 K^+ channels causes epilepsy. Nature 396:687–690

Schroeder BC, Hechenberger M, Weinreich F, Kubisch C, Jentsch TJ (2000) KCNQ5, a novel potassium channel broadly expressed in brain, mediates M-type currents. J Biol Chem 275:24089–24095

Schwake M, Pusch M, Kharkovets T, Jentsch TJ (2000) Surface expression and single channel properties of KCNQ2/KCNQ3, M-type K^+ channels involved in epilepsy. J Biol Chem 275:13343–13348

Selyanko AA, Hadley JK, Wood IC, Abogadie FC, Delmas P, Buckley NJ, London B, Brown DA (1999) Two types of K^+ channel subunit, Erg1 and KCNQ2/3, contribute to the M-like current in a mammalian neuronal cell. J Neurosci 19:7742–7756

Singh NA, Westenskow P, Charlier C, Pappas C, Leslie J, Dillon J BFNC Physician Consortium, Anderson VE, Sanguinetti MC, Leppert MF (2003) KCNQ2 and KCNQ3 potassium channel genes in benign familial neonatal convulsions: expansion of the functional and mutation spectrum. Brain 126:2726–2737

Soldovieri MV, Castaldo P, Iodice L, Miceli F, Barrese V, Bellini G, Miraglia del Giudice E, Pascotto A, Bonatti S, Annunziato L, Taglialatela M (2006) Decreased subunit stability as a novel mechanism for potassium current impairment by a KCNQ2 C terminus mutation causing benign familial neonatal conclusions. J Biol Chem 280:418–428

Wang HS, Pan Z, Shi W, Brown BS, Wymore RS, Cohen IS, Dixon JE, McKinnon D (1998) KCNQ2 and KCNQ3 potassium channel subunits: molecular correlates of the M-channel. Science 282:1890–1893